

# Measurements of the angle $\alpha$ ( $\phi_2$ ) at *BABAR*

Sandrine Emery <sup>a</sup>

On behalf of the *BABAR* collaboration

<sup>a</sup>CEA-Saclay, DAPNIA/SPP  
91191 Gif-sur-Yvette, France

Measurements of the angle  $\alpha$  ( $\phi_2$ ) of the Unitarity Triangle from the *BABAR* experiment are presented. The measurements are based on about 230 million  $B\bar{B}$  pairs where one  $B$  meson decays into two pions, two rhos, or three pions (Dalitz analysis). These three measurements yield a combined value of  $\alpha = (103_{-9}^{+11})^\circ$ .

## 1. Physics motivation

In the Standard Model, CP violation in the quark sector is due to the complex  $V_{CKM}$  matrix relating the quark weak eigenstates to their mass eigenstates. One unitarity condition can be written as the Unitarity Triangle:  $V_{ud}V_{ub}^* + V_{cd}V_{cb}^* + V_{td}V_{tb}^* = 0$ . Over-constraining this triangle allows one to search for inconsistencies in the Standard Model. Its angles are generally measured in CP-violating processes. The angle  $\beta$  is the phase of  $V_{td}$  accessible in  $B^0\bar{B}^0$  mixing, and has already been measured precisely at the  $B$  factories. The angle  $\gamma$  is the phase of  $V_{ub}$  found in  $b \rightarrow u$  transitions like  $B \rightarrow \pi\pi$ ,  $\rho\rho$ , or  $\rho\pi$ . The angle  $\alpha = \pi - \beta - \gamma$  can be extracted in processes that involve both  $B^0\bar{B}^0$  mixing and  $b \rightarrow u$  transitions.

## 2. Extraction of $\alpha$ in $B \rightarrow \pi\pi, \rho\rho$ decays.

### 2.1. Time-dependent CP asymmetry.

A  $B^0$  meson can decay into a final CP eigenstate  $f_{CP}$ , like  $\pi^+\pi^-$  or  $\rho^+\rho^-$ , either directly with an amplitude  $A_{f_{CP}}$ , or after having mixed to a  $\bar{B}^0$  meson with an amplitude  $\frac{q}{p} \times \bar{A}_{f_{CP}}$ , where  $q$  and  $p$  relate the  $B$ -mesons mass eigenstates to their flavor eigenstates:  $|B_L\rangle = p|B^0\rangle + q|\bar{B}^0\rangle$ ,  $|B_H\rangle = p|B^0\rangle - q|\bar{B}^0\rangle$ . As CP violation in the mixing itself is negligible,  $\frac{|p|}{|q|} \simeq 1$  and  $\frac{q}{p} \simeq e^{-i2\beta}$ . The study of the time dependent CP asymmetry:

$$a_{f_{CP}}(\Delta t) = \frac{\Gamma(\bar{B}^0 \rightarrow f_{CP}) - \Gamma(B^0 \rightarrow f_{CP})}{\Gamma(\bar{B}^0 \rightarrow f_{CP}) + \Gamma(B^0 \rightarrow f_{CP})} \quad (1)$$

$$= S_{f_{CP}} \sin(\Delta m_d \Delta t) - C_{f_{CP}} \cos(\Delta m_d \Delta t)$$

allows one to measure  $S_{f_{CP}}$  and  $C_{f_{CP}}$  which are functions of the ratio  $\lambda_{f_{CP}} = \frac{q}{p} \times \frac{\bar{A}_{f_{CP}}}{A_{f_{CP}}}$  of the  $B^0$  decay amplitudes with and without mixing:  $S_{f_{CP}} = \frac{2\Im(\lambda_{f_{CP}})}{1+|\lambda_{f_{CP}}|^2}$ ,  $C_{f_{CP}} = \frac{1-|\lambda_{f_{CP}}|^2}{1+|\lambda_{f_{CP}}|^2}$ . Note that  $C_{f_{CP}} \neq 0$  only if  $\frac{|\bar{A}_{f_{CP}}|}{|A_{f_{CP}}|} \neq 1$ , i.e. in the presence of direct CP violation. While  $S_{f_{CP}} \neq 0$  can occur without direct CP violation, its value is affected by direct CP violation.

$B^0 \rightarrow h^+h^-$  decays ( $hh = \pi\pi, \rho\rho$ ) are dominated by the  $b \rightarrow u$  tree amplitude  $T$ , with weak phase  $\gamma$ . Ignoring other contributions, one would simply get  $\lambda_{h^+h^-} = \frac{q}{p} \times \frac{\bar{T}}{T} = e^{-i2\beta} e^{-i2\gamma} = e^{i2\alpha}$ ,  $C_{h^+h^-} = 0$  and  $S_{h^+h^-} = \sin(2\alpha)$ . But contributions of amplitude  $P$ , from dominant gluonic penguins and with no weak phase, allow direct CP violation. If we define the amplitude  $T'$  as that dominated by tree processes but also including non-dominant penguins with a weak phase  $\gamma$ , and if  $\delta$  is the strong phase difference between the  $T'$  and  $P$  amplitudes then:  $\lambda_{h^+h^-} = e^{i2\alpha} \frac{|T'|+|P|e^{+i\gamma}e^{i\delta}}{|T'|+|P|e^{-i\gamma}e^{i\delta}}$ ,  $C_{h^+h^-} \propto \sin\delta$ , and  $S_{h^+h^-} = \sqrt{1-C^2} \times \sin(2\alpha_{eff})$ . Measuring  $C_{h^+h^-}$  and  $S_{h^+h^-}$  only yields an effective value of  $\alpha$ ,  $\alpha_{eff}$ , which depends on the  $B$ -decay mode studied.

## 2.2. The isospin analysis

Fortunately, other  $B$ -mesons decays to  $hh$  can be used to determine the difference  $\alpha - \alpha_{eff}$  using isospin symmetry [1]. Tree and penguin contributions to  $hh$  decays are summarized in Table 1. Since the tree amplitude in the  $B^0 \rightarrow h^0 h^0$  decays is color suppressed and of the same order of magnitude as the penguin amplitude, the branching ratio of these modes is expected to be small. Also the isospin conservation rules exclude gluonic penguin transitions for isospin-even  $h^+ h^0$  final states. These modes are then pure tree decays, though the  $\rho^+ \rho^0$  final state could have a slight isospin 1 contribution due to the wide  $\rho$  resonances [2]. The  $SU(2)$  isospin symmetry relates

Table 1

Mode	Tree	Penguin
$h^+ h^-$	Color-allowed	Present
$h^0 h^0$	Color-suppressed	Present
$h^+ h^0$	Color-allowed	Forbidden

the amplitudes of all the  $hh$  modes. Moreover, the amplitude of the pure tree  $h^+ h^0$  mode is equal to that for its charge conjugate process. We define  $A^{+-} = A(B^0 \rightarrow h^+ h^-)$ ,  $A^{+0} = A(B^+ \rightarrow h^+ h^0)$ ,  $A^{00} = A(B^0 \rightarrow h^0 h^0)$ , with the symbol  $\tilde{\phantom{A}}$  for the charge conjugate processes. Neglecting electroweak penguins and  $SU(2)$ -breaking effects, we obtain:

$$\frac{A^{+-}}{\sqrt{2}} + A^{00} = A^{+0} = \tilde{A}^{-0} = \frac{\tilde{A}^{+-}}{\sqrt{2}} + \tilde{A}^{00}. \quad (2)$$

These relationships are represented as two triangles with a common base, as shown in Figure 1. Measuring the lengths of the sides of the two triangles, or the branching ratios of the various modes, constrains  $\alpha - \alpha_{eff}$ .

## 3. BABAR analyses

Three analyses are discussed. A combined constraint on  $\alpha$  will be shown at the end.

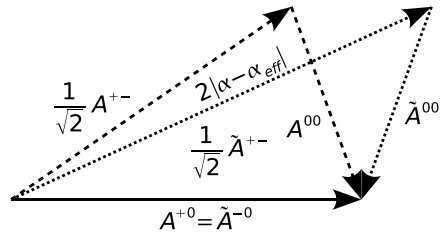


Figure 1. Isospin relationships.

### 3.1. Common features of analyses

The *BABAR* detector is described in details in [3].  $B\bar{B}$  pairs resulting from the  $\Upsilon(4S)$  decays are produced in a coherent state. The CP asymmetry is measured as a function of the difference  $\Delta t = \gamma\beta\Delta z$  between the two  $B$ -mesons decay times which is proportional to  $\Delta z$ , the difference between their flight distances due to a boost of  $\gamma\beta \approx 0.56$  given to the  $\Upsilon(4S)$ . The average  $\Delta z$  is around  $250 \mu\text{m}$ , with a resolution of about  $170 \mu\text{m}$ . One of the  $B$  mesons is fully reconstructed into the  $B$  decay of interest ( $\pi\pi$ ,  $\rho\rho$ , or  $\pi\pi\pi$ ), while the other  $B$  meson is used to tag its flavor at production time. Tagging combines different techniques including the use of semileptonic decays and secondary kaons. The  $B$ -flavor tagging power  $Q = \sum_i \epsilon_i (1 - 2\omega_i)^2$  is close to 30%, when summed over the different tagging categories  $i$ , with efficiencies  $\epsilon_i$  and mistag rates  $\omega_i$ .

To select the signal, hadron identification is used to separate pions from kaons. The beam energy ( $E_{beam}$ ) substituted mass  $m_{ES} = \sqrt{E_{beam}^{*2} - p_B^{*2}}$ , and the energy difference  $\Delta E = E_B^* - E_{beam}^*$  are powerful kinematic discriminating variables, peaking respectively for the signal at the  $B$ -meson mass and zero. The symbol  $*$  refers to the  $\Upsilon(4S)$  rest frame. The largest background consists of  $q\bar{q}$  ( $q = u, d, s, c$ ) continuum events. The  $B\bar{B}$  events look spherical while the continuum events are jet-like, so event shape variables are also used for separation. The variables are combined into one using either a Fisher discriminant or a neural network. The following results are based on a multi-variable maximum like-

likelihood analysis of the quasi-independent observables  $m_{ES}$ ,  $\Delta E$ , and the Fisher discriminant or neural net output.

### 3.2. Results from $B \rightarrow \pi\pi$ decays

The time-dependent CP asymmetry of the  $B^0 \rightarrow \pi^+\pi^-$  decays has been studied using  $227 \times 10^6$   $B\bar{B}$  pairs [4]. A fit that includes  $467 \pm 33$  reconstructed signal events gives a measurement of  $S_{\pi\pi} = -0.30 \pm 0.17 \pm 0.03$  and  $C_{\pi\pi} = -0.09 \pm 0.15 \pm 0.04$ , consistent with no direct CP violation. The errors are statistics limited.

The branching ratios of the various  $\pi\pi$  modes are needed to perform an isospin analysis. The branching ratio  $BR(B^0 \rightarrow \pi^+\pi^-) = [4.7 \pm 0.6 \pm 0.2] \times 10^{-6}$  was measured earlier using  $88 \times 10^6$   $B\bar{B}$  pairs [5], and was updated after this conference [6]. The branching ratios of the  $B^0 \rightarrow \pi^0\pi^0$  and  $B^+ \rightarrow \pi^+\pi^0$  modes, as well as those of their charge conjugate processes, have been measured using  $227 \times 10^6$   $B\bar{B}$  pairs [7]. The average branching ratios  $BR$  over the charge conjugate processes, as well as the time-integrated charge asymmetries  $C$  are:  $BR_{00} = [1.17 \pm 0.32 \pm 0.10] \times 10^{-6}$ ,  $C_{00} = -0.12 \pm 0.56 \pm 0.06$ ,  $BR_{+0} = [5.8 \pm 0.6 \pm 0.4] \times 10^{-6}$ ,  $C_{+0} = -0.01 \pm 0.10 \pm 0.02$ . The  $B^0 \rightarrow \pi^0\pi^0$  branching ratio is small but much larger than theoretical expectations. It was observed with a  $5.0 \sigma$  significance. The final constraints on  $\alpha$  are not strong enough to derive a measurement (see Sec. 4).

### 3.3. Results from $B \rightarrow \rho\rho$ decays

$B \rightarrow \rho\rho$  analyses are experimentally more challenging than the  $B \rightarrow \pi\pi$  analyses as the final states consist of four pions, including two  $\pi^0$  for the  $\rho^+\rho^-$  mode. The wide  $\rho$  resonances result in more background. These vector-vector modes are also not CP eigenstates. But as they are almost 100% longitudinally polarized, an analysis of the sole longitudinal (CP-even) component is adequate. On the other hand, the  $B \rightarrow \rho\rho$  branching ratio is about 6 times larger than for  $B \rightarrow \pi\pi$ , and the penguin pollution is much smaller as we will see. Thus this mode is better for constraining  $\alpha$  (see Sec. 4). A similar analysis to that for  $\pi^+\pi^-$  is performed for the  $\rho^+\rho^-$  mode in [8], with the

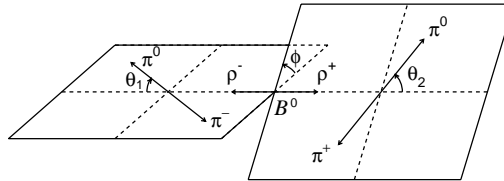


Figure 2.  $B^0 \rightarrow \rho^+\rho^-$  decay helicity frame.

reconstructed masses of the two  $\rho$ s as well as their helicity angles as additional observables, and the fraction  $f_L$  of longitudinal polarization as an additional parameter. The decay rate as a function of  $f_L$  and the helicity angles  $\theta_{1,2}$  (Fig. 2) is:  $\frac{d\Gamma}{d\theta_1 d\theta_2} \propto \frac{1-f_L}{4} \sin^2 \theta_1 \sin^2 \theta_2 + f_L \cos^2 \theta_1 \cos^2 \theta_2$

Using  $232 \times 10^6$   $B\bar{B}$  pairs, we obtain  $f_L = 0.978 \pm 0.014^{+0.021}_{-0.029}$ . For the longitudinal component, we have  $S_L^{\rho^+\rho^-} = -0.33 \pm 0.24^{+0.08}_{-0.14}$  and  $C_L^{\rho^+\rho^-} = -0.03 \pm 0.18 \pm 0.09$ .

The  $617 \pm 52$  signal events found are consistent with the previous measurement of the branching ratio [9] of  $[30 \pm 4 \pm 5] \times 10^{-6}$  using  $89 \times 10^6$   $B\bar{B}$  pairs. To perform the isospin analysis, a lower limit of  $1.1 \times 10^{-6}$  at 90% confidence level on  $BR(B^0 \rightarrow \rho^0\rho^0)$  [10] was measured recently, assuming this mode is purely longitudinal (the most conservative limit). The largest systematics is due to the potential interference with  $a_1^\pm \pi^\mp$  (22%). An isospin analysis is also presented in [10], using the average of old Belle [12] and BABAR [11] results for the  $\rho^+\rho^0$  mode:  $BR(B^+ \rightarrow \rho^+\rho^0) = [26.4 \pm 6.4] \times 10^{-6}$  and  $f_L(\rho^+\rho^0) = 0.96^{+0.05}_{-0.07}$ . The small value of the  $\rho^0\rho^0$  branching ratio compared to the one for the pure tree  $\rho^+\rho^0$  mode shows that the penguin contributions are small in the  $\rho\rho$  modes.

The most probable solution for  $\alpha$  is  $(100 \pm 13)^\circ$ . (See Sec. 4).

### 3.4. $B^0 \rightarrow \pi^+\pi^-\pi^0$ Dalitz analysis.

The  $B^0 \rightarrow \rho^+\pi^+$  decay has no final CP eigenstate like  $\pi^+\pi^-$  or  $\rho^+\rho^-$ . An isospin analysis would not constrain sufficiently the many amplitudes of the  $B^{0,+}$  decays to  $\rho^+\pi^-$ ,  $\rho^-\pi^+$ ,  $\rho^0\pi^0$ ,  $\rho^+\pi^0$ ,  $\rho^0\pi^+$  and their charge conjugates. A better approach [13] is based on the time-dependent

analysis of the  $B^0 \rightarrow \pi^+\pi^-\pi^0$  decay over the Dalitz plot, using the isospin symmetry as an additional constraint. As this  $B \rightarrow 3\pi$  decay is dominated by  $\rho\pi$  resonances (Fig. 3), its ampli-

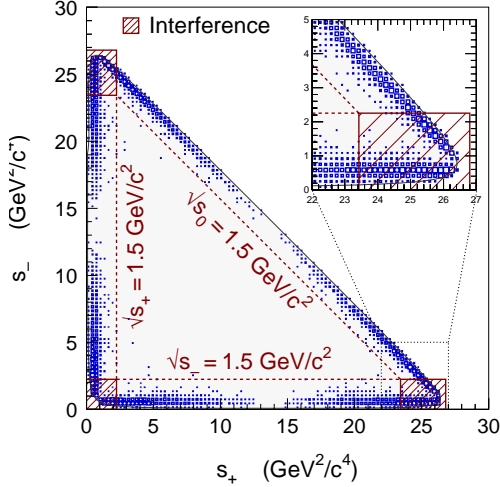


Figure 3. Dalitz plot for  $B^0 \rightarrow \pi^+\pi^-\pi^0$  decays.

tude is a function of well-known kinematic functions of the Dalitz variables and of the  $B^0 \rightarrow \rho\pi$  amplitudes, themselves functions of  $\alpha$  and tree and penguin contributions:  $A(B^0 \rightarrow \rho^\kappa\pi^{-\kappa}) = T^\kappa e^{-i\alpha} + P^\kappa$  ( $\kappa=(0, +, -)$ ). Only the sign of the weak phase  $\alpha$  is changed when switching to the charge conjugate process. The time-dependent CP analysis of the  $B^0 \rightarrow \pi^+\pi^-\pi^0$  decay then provides enough constraints to extract  $\alpha$  and the tree and penguin amplitudes. This measurement has been done at *BABAR* [14] using  $213 \times 10^6 B\bar{B}$  pairs, giving a value of  $\alpha = (113_{-17}^{+27} \pm 6)^\circ$ .

#### 4. Summary of the *BABAR* results on $\alpha$

Figure 4 [15] summarizes all constraints on  $\alpha$  obtained at *BABAR*, yielding a combined value of  $\alpha = (103_{-9}^{+11})^\circ$  in good agreement with the global CKM fit using other world measurements. The  $\rho\rho$  mode gives the best single measurement, but has mirror solutions that are disfavored thanks to the Dalitz analysis results. The contribution to the constraint from the  $\pi\pi$  modes is limited, mostly due to the large penguin pollution.

Accuracy will improve in the future with more data, and with updates of the  $\rho^+\rho^0$  and  $\rho^+\rho^-$  branching ratios using our full data sample. The measurement of the  $\rho^0\rho^0$  branching ratio is the limiting factor. When the  $\rho^0\rho^0$  channel is observed, a time-dependent CP analysis could also provide additional constraints. New Belle results using the  $\rho\rho$  mode [16] shown shortly after this conference are in good agreement with *BABAR*.

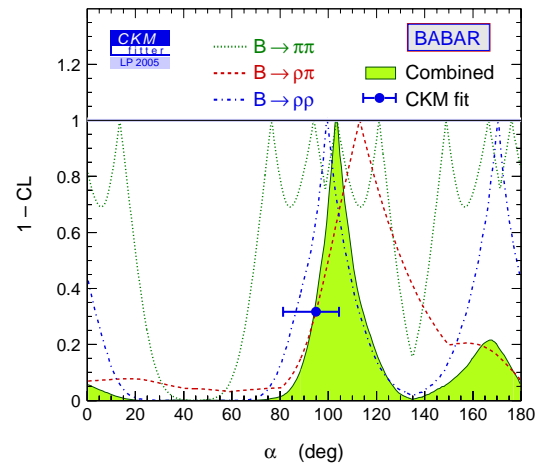


Figure 4. Confidence level versus  $\alpha$  for all modes.

#### REFERENCES

1. Gronau, London, PRL 65, 3381 (1990).
2. Falk *et al.* hep-ph/0310242.
3. *BABAR* collab., NIM A 479:1-116 (2002).
4. *BABAR* collab., hep-ex/0501071, sub. to PRL.
5. *BABAR* collab., PRL 89, 281802 (2002).
6. *BABAR* collab., hep-ex/0508046.
7. *BABAR* collab., PRL 94, 181802 (2005).
8. *BABAR* collab., PRL 95, 041805 (2005).
9. *BABAR* collab., PRL 93, 231801 (2004).
10. *BABAR* collab., PRL 94, 131801 (2005).
11. *BABAR* collab., PRL 91, 171802 (2003).
12. Belle collab., PRL 91, 221801 (2003).
13. Snyder, Quinn, PRD 48, 2139 (1993).
14. *BABAR* collab., hep-ex/0408099.
15. <http://ckmfitter.in2p3.fr> (Moriond 2005).
16. Belle collab., hep-ex/0507039.